Regular and anomalous Extraordinary Optical Transmission at the THz-gap

S.A. Kuznetsov[1,2], M. Navarro-Cía[3],V.V. Kubarev[2], A.V. Gelfand[4], M. Beruete[3], I. Campillo[5], and M. Sorolla[3*]

[1] *Novosibirsk State University, Research-and-Education Centre "Nanosystems and Modern Materials", Pirogova Str. 2, 630090 Novosibirsk, Russia*
[2] *Budker Institute of Nuclear Physics SB RAS, Lavrentiev Ave. 11, 630090 Novosibirsk, Russia*
[3] *Millimeter and Terahertz Waves Laboratory, Universidad Pública de Navarra, Campus Arrosadía, 31006 Pamplona, Spain*
[4] *Institute of Semiconductor Physics SB RAS, Novosibirsk Branch "TDIAM", Nikolaeva Str. 8, 630090 Novosibirsk, Russia*
[5] *CIC nanoGUNE Consolider, Tolosa Hirbidea 76, 20018 Donostia, Spain*
[*] *mario@unavarra.es*

Abstract: In this paper Anomalous Extraordinary Transmission (ET) is reported for s-polarization of low loss doubly periodic subwavelength hole arrays patterned on polypropylene (PP) substrates by conventional contact photolithography at the so-called THz-gap (1-10 THz). The unexpected enhanced transmittance for s-polarization (i.e. without spoof plasmons) was previously numerically demonstrated in subwavelength slits arrays. However, subsequently no experimental work has been devoted to this unexpected Extraordinary Transmission neither in subwavelength slits nor in subwavelength holes. Here, numerical study and experimental results of the Anomalous ET and the symmetric and antisymmetric transmittance modes associated with the already well-known p-polarization ET are shown alongside a systematically analysis of the frequency peaks as a function of hole size for both incident polarizations.

OCIS codes: (999.9999) Extraordinary Transmission; (040.2235) Far infrared or terahertz; (050.6624) Subwavelength structures; (240.6680) Surface plasmons; (050.6624) Surface waves;

References and links

1. J. Rayleigh, "On the dynamical theory of gratings," Proc. R. Soc. London A **79**, 399-416 (1907).
2. E. H. Synge, "A suggested model for extending microscopic resolution into the ultra-microscopic region," Philos. Mag. **3**, 356-362 (1928).
3. A. Lewis, M. Isaacson, A. Harootunian, and A. Muray, "Development of a 500Å resolution microscope," Ultramicroscopy **13**, 227-231 (1984).
4. H. A. Bethe, "Theory of diffraction by small holes," Phys. Rev. **66**, 163-182 (1944).
5. R. Ulrich, "Far–infrared properties of metallic mesh and its complementary structure," Inf. Phys. **7**, 37-55, (1967).
6. C. C. Chen, "Transmission of Microwave Through Perforated Flat Plates of Finite Thickness," IEEE Trans. Microwave Theory Tech. **21**, 1-7, (1973).
7. T. W. Ebbesen, H. J. Lezec, H. Ghaemi, T. Thio, and P. A. Wolf, "Extraordinary optical transmission through sub-wavelength hole arrays," Nature **391**, 667-669 (1998).
8. M.M.J. Treacy, "Dynamical diffraction in metallic optical gratings," Appl. Phys. Lett. **75**, 606-608 (1999).
9. J.A. Porto, F.J. García-Vidal, J.B. Pendry, "Transmission resonances on metallic gratings with very narrow slits," Phys. Rev. Lett. **83**, 2845–2848 (1999).
10. H. J. Lezec, A. Degiron, E. Devaux, R. A. Linke, L. Martín-Moreno, F. J. García-Vidal, and T. W. Ebbesen, "Beaming light from a subwavelength aperture," Science **297**, 820–822 (2002).
11. L. Martín-Moreno, F. J. García-Vidal, H. J. Lezec, K. M. Pellerin, T. Thio, J. B. Pendry, and T. W. Ebbesen, "Theory of Extraordinary Optical Transmission through Subwavelength Hole Arrays," Phys. Rev. Lett. **86**, 1114-1117 (2001).

#109149 - $15.00 USD Received 25 Mar 2009; revised 7 May 2009; accepted 3 Jun 2009; published 29 Jun 2009

12. M. Beruete, M. Sorolla, I. Campillo, J. S. Dolado, I. Martín-Moreno, J. Bravo-Abad, and F. J. García-Vidal, "Enhanced millimetre-wave transmission through subwavelength hole arrays," Opt. Lett. **29** 2500-2502 (2004).
13. M. Sarrazin, J. P. Vigneron and J. M. Vigoureux, "Role of Wood anomalies in optical properties of thin metallic films with a bidimensional array of subwavelength holes," Phys. Rev. B **67**, 085415-1-8 (2003).
14. V. Lomakin and E. Michielssen, "Enhanced transmission through metallic plates perforated by arrays of subwavelength holes and sandwiched between dielectric slabs," Phys. Rev. B **71**, 235117-1-10 (2005).
15. D. R. Jackson, A. A. Oliner, T. Zhao, and J. T. Williams, "Beaming of light at broadside through a subwavelength hole: Leaky wave model and open stopband effect," Radio Sci. **40**, 1-12 (2005).
16. J. B. Pendry, L. Martín-Moreno, and F. J. García-Vidal, "Mimicking Surface Plasmons with Structured Surfaces," Science **305**, 847-848 (2004).
17. M. Beruete, I. Campillo, J. E. Rodríguez-Seco, E. Perea, M. Navarro-Cía, I. J. Núñez-Manrique, and M. Sorolla, "Enhanced Gain by Double-Periodic Stacked Subwavelength Hole Array," IEEE Microwave Wireless Compon. Lett. **17**, 831-833 (2007).
18. J. Gómez Rivas, C. Schotsch, P. Haring Bolivar, and H. Kurz, "Enhanced transmission of THz radiation through subwavelength holes," Phys. Rev. B **68**, 201306-1-4 (2003).
19. E. Hendry, M. J. Lockyear, J. Gómez Rivas, L. Kuipers, and M. Bonn, "Ultrafast optical switching of the THz transmission through metallic subwavelength hole arrays," Phys. Rev. B **75**, 235305-1-5 (2007).
20. A. K. Azad, Y. Zhao, W. Zhang, and M. He, "Effect of dielectric properties of metals on terahertz transmission in subwavelength hole arrays," Opt. Lett. **31**, 2637-2639 (2006).
21. E. Moreno, L. Martín-Moreno, and F. J. García-Vidal, "Extraordinary optical transmission without plasmons: the s-polarization case," J. Opt. A: Pure Appl. Opt. **8**, S94–S97 (2006).
22. M. Beruete, M. Sorolla, M. Navarro-Cía, F. Falcone, I. Campillo, and V. Lomakin, "Extraordinary transmission and left-handed propagation in miniaturized stacks of doubly periodic subwavelength hole arrays," Opt. Express **15**, 1107-1114 (2007).
23. M. Aznabet, M. Navarro-Cía, S. A. Kuznetsov, A. V. Gelfand, N. I. Fedorinina, Yu. G. Goncharov, M. Beruete, O. El Mrabet, and M. Sorolla, "Polypropylene-substrate-based SRR- and CSRR- metasurfaces for submillimeter waves," Opt. Express **16**, 18312-18319 (2008).
24. A. Krishnan, T. Thio, T. J. Kim, H. J. Lezec, T. W. Ebbesen, P. A. Wolff, J. Pendry, L. Martín-Moreno, and F. J. García-Vidal, "Evanescently coupled resonance in surface plasmon enhanced transmission," Opt. Commun. **200**, 1-7 (2001).
25. K. L. van der Molen, F. B. Segerink, N. F. van Hulst, and L. Kuipers "Influence of hole size on the extraordinary transmission through subwavelength hole arrays," Appl. Phys. Lett. **85**, 4316-4318 (2004).

1. Introduction

The band between 1 THz and 10 THz (0.3-0.03 mm), so-called Terahertz-gap, is a region of the spectrum where many molecular excitations, such as rotations and vibrations, happen. Moreover, THz electromagnetic waves can penetrate through several optical opaque materials and biological tissues, and thus allow their use for imaging in both security and medical applications. Therefore, this range has a huge potential not only for physical characterization, but for chemical analysis as well.

Early study of transmission through subwavelength holes has its origin at the beginning of 20th century [1]. Later on, Synge [2] proposed the use of a small aperture close to the sample surface to overcome the diffraction limit, but it was not applied until mid 80's in the development of near-field scanning optical microscopy [3] using arrays of subwavelength holes. Contrary to Bethe's theoretical model [4] of the 40's, these arrays gave rather significant enhanced transmission. In parallel, microwave transmission through periodically perforated thin metallic plates had been studied since 60's. [5, 6]. However, it was Ebbesen *et al.* [7] who paid particular attention to the high transmittance peaks observed at optical wavelengths within the cutoff defined by the aperture size of perforated plates, namely Extraordinary Optical Transmission (EOT) (it is worth noting that also anomalous high transmittance was reported in subwavelength slit arrays [8,9] and a subwavelength slot in corrugated surfaces [10], but from now on, we will not deal with them). This enhancement was successfully explained in terms of Surface Plamons Polaritons (SPPs), but subsequent analytical results under Perfect Conductor condition [11] and experimental results in perforated aluminum plates at millimeter-waves [12], where metals no longer support SPPs, brought some doubts about the physics underlying the EOT. Therefore, explanations based on Wood's anomaly [13,14] and leaky waves formalism started to become important [15]. Finally, Pendry *et al.* [16] found that perforated periodically subwavelength holes change the

#109149 - $15.00 USD Received 25 Mar 2009; revised 7 May 2009; accepted 3 Jun 2009; published 29 Jun 2009

effective electric permeability of the metal, in such a way that it behaves as an electron plasma, being also consistent with the far-field reflection and dispersion experiments. They termed the wave supported in that structured surface as spoof plasmon.

Extensive experimental research of EOT in microwaves [17], millimeter-waves [12] and optics [7] has been carried out, but few analyses [18-20] have been devoted to the so-called THz-gap. A couple of these papers was dedicated to perforated doped semiconductor [18,19], whereas the other one dealt with perforated metallic plates and provides a deep investigation of the influence of the dielectric properties of metals [20].

Nevertheless, this is not the whole of the story. In 2006 a paper was published showing numerically EOT for s-polarization (i.e. without spoof plasmons) in subwavelength slit arrays lying over a thin dielectric layer, which plays a key role for the unexpected enhancement [21]. Here we report for the first time the experimental realization at the THz-gap of this anomalous high transmittance. Similar results but in millimeter wave range can be found in [22] despite this feature was not claimed. Also, Ulrich reported analogous resonances but for inductive grid with propagating holes [5].

This paper demonstrates experimentally the anomalous EOT for s-polarized excitation (electric field along the short periodicity, E_x). Also, it triggers intensive discussion on design, low-cost manufacture and measurement of EOT doubly periodic subwavelength hole arrays in metallic surfaces on/over Polypropylene substrates within THz-gap. Furthermore, experimental verification of both symmetric and antisymmetric modes, that were not previously reported in this THz cutoff range, as well as analysis of hole size dependence of transmittance are presented.

2. "THz-performance" of polypropylene substrates and design of THz-EOT prototypes

At terahertz frequencies typical topological sizes of EOT-structures become of the order of ~10–100μm that is very suitable for creating a topological micro-pattern by a well-tailored contact photolithography technique (CPhLT) employed in the semiconductor industry. The key problem of non-self-bearing THz-structures is the lack of appropriate low absorbing and low dispersive substrates fitting for CPhLT. It should be noted that frequently used polyimide-based (PI-based) substrates obtained by high-quality PI-film growing from a liquid phase due to spin coating and subsequent thermal annealing processes are considered to be ideal for CPhLT; PI has high stiffness, minimal inner and surface defects and its thickness can be accurately controlled. However, the fundamental drawback of PI limiting its use in THz-applications is absorption which is undesirably high even at small values of thickness (a few microns). In comparison with PI, polypropylene (PP) and polyethylene (PE) exhibit in general drastically smaller losses and dispersion within the THz-band which, along with their relative cheapness and commercial availability makes them very promising substrate materials for applied THz-sciences and engineering. Unlike PE, PP is considered to be a more "technological" material due to its higher mechanical fastness, melting temperature and better chemical adhesion. In our recent works we have successfully adapted CPhLT for creating PP-based mesh filters and metasurfaces for millimetre and submillimetre waves ($f \approx$ 45-500 GHz) [23]. In this work we extended CPhLT for fabricating structures with smaller scale topologies – topologies of EOT hole arrays with EOT-resonance at frequencies ~2-3 THz. The main drawback of commercial PP (as well as PE) follows from its production technology – extrusion from a hot liquid melt of polymeric microgranules that may lead to uncontrollable deviation of thickness (up to 20%) and increase number of film microdefects. In particular, the latter effect is manifested, as we show below, in the appearance of microhillocks on the PP-film surface with typical height of a microgranule size. On average the microhillocks do not deteriorate THz-transmission of the film, but may result in some deviation of the topological dimensions of the microstructures fabricated by CPhLT due to a loose contact between the film and the photo-mask.

Figure 1 presents the results of wideband Fourier-transform THz-characterization of some commercial PP-films with different thickness (the values are pointed in the insets). The case of 4μm-thick PI-film is shown in Fig. 1(a) for comparison. The data overlap the band 1.5-21

#109149 - $15.00 USD Received 25 Mar 2009; revised 7 May 2009; accepted 3 Jun 2009; published 29 Jun 2009

THz and were obtained using the vacuum FT-spectrometer "Bruker IFS 66v/s" (spectral resolution ~0.1 cm^{-1}) under "room temperature" measurement conditions. The results show high transmittance of PP-films for moderate values of thickness (8-40μm). Derived from the presented graphs the averaged values of PP's optical constants (for the points far from molecular absorption bands at 398, 459 and 529 cm^{-1}) are close to the following: refractive index $n \approx 1.5 \pm 0.02$, loss tangent $tg\delta \approx 1\text{-}1.5 \cdot 10^{-3}$. The constants exhibit very small frequency dispersion within the investigated THz-band; a slight difference is revealed for film samples from different PP-suppliers: e.g. our 39μm-PP-sample exhibits higher values of n and $tg\delta$ than the 40μm-one, which is clearly seen from position and magnitude of Fabry-Perot resonances in spectral transmission (s-polarization 1(c)).

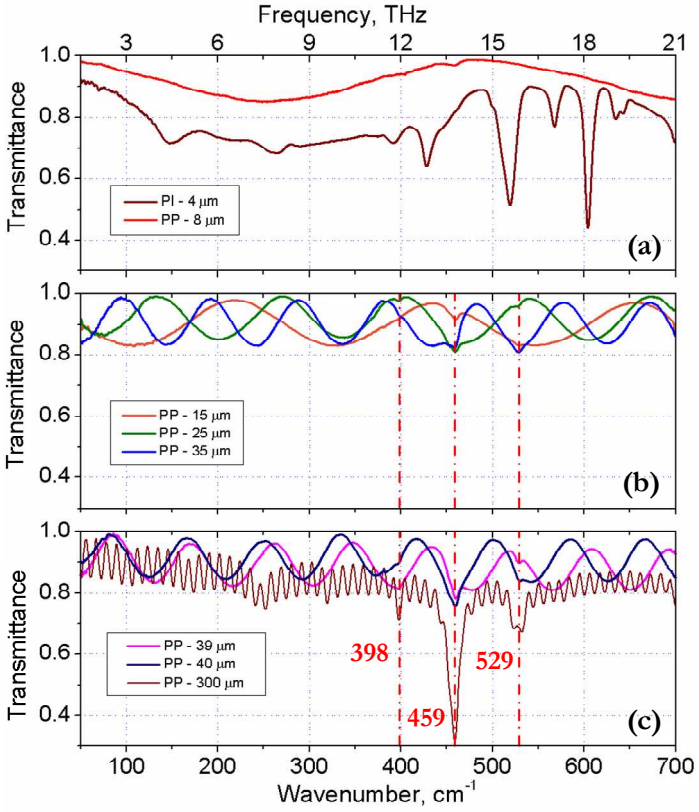

Fig. 1. Optical properties of PP-films at terahertz frequencies. THz-transmittance of 4μm-thick PI-film (a) is shown for comparison. Dashed lines with numbers (b, c) indicate positions of most intensive PP absorption lines. Note that we use the abscissas in both wavenumber (bottom in cm^{-1}) and frequency (top in THz) units.

To fabricate terahertz EOT hole array prototypes discussed in this paper we have chosen a 20μm-thick PP-film estimated to be a compromise between the requirements of thickness minimization (to decrease dielectric losses) and appropriate stiffness (acceptable for employed CPhLT procedures), see details in Fig. 2. In addition, a microscopic study revealed fewer granularity of such a film compared to close in parameters 15μm-thick PP-film from our set of available thicknesses. The design parameters for 20μm-PP-based asymmetric EOT hole arrays were chosen to set the EOT-resonances at 2 and 2.6 THz (not far from the low-frequency end of the instrumentation band) that defined the following values: transversal periodicities d_x = 47.5 μm and d_y = 113 μm, hole diameter a = 40.1 μm, aluminum metallization thickness t = 0.5 μm (a unit cell is shown in Fig. 2(a)). It is well-known that

#109149 - $15.00 USD Received 25 Mar 2009; revised 7 May 2009; accepted 3 Jun 2009; published 29 Jun 2009

asymmetric prototypes (prototypes with different dielectrics in each interface) have a worst performance in terms of transmittance [14,24] since SPP-like waves excited in either side of the metal have different frequencies and therefore, the perfect matching between them is lost, yielding to less transmittance. In consequence, a doubly periodic subwavelength hole array has been designed to minimize in somehow this problem.

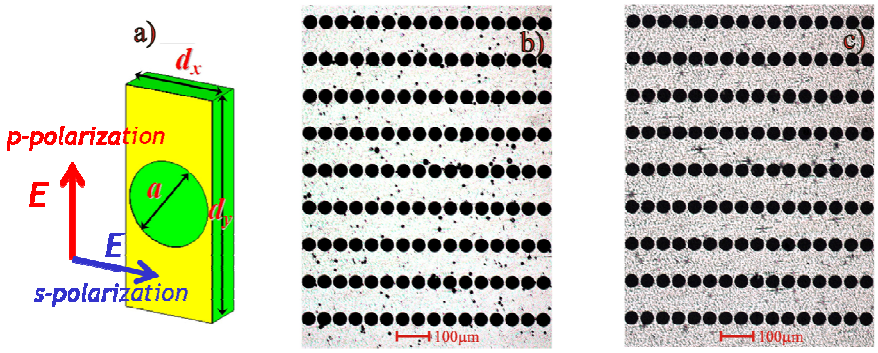

Fig. 2. (a): Geometry of hole array unit cell. Note that the PP is not perforated (b, c): Microscope images of 20μm-PP-film-backed hole arrays (prototype #3) illustrating inherent granularity (surface roughness) of low-cost commercial PP-films. The case (b) corresponds to focusing on the nearest PP surface, the case (c) – focusing on the top of microhillocks.

Table 1. Key information of fabricated prototypes

Prototype	Metallization	Measured hole diameter, *a*
#1	0.5μm-Al	39.75μm ± 0.15μm
#2	0.5μm-Al	40.95μm ± 0.25μm
#3	20nm-Ti + 0.5μm-Al	41.35μm ± 0.15μm
#4	20nm-Ti + 0.5μm-Al *(preliminary heating of PP-film at 100^0C)*	43.1μm ± 0.05μm

CPhLT, whose stages are described in [23], was used to fabricate four hole array prototypes with 50 mm clear aperture diameter. For two of them before thermal deposition of Al onto PP an auxiliary thin (20nm-thick) layer of Titanium (Ti) was created by magnetron sputtering to study enhancement of surface adhesion of Al to PP. Our technological experiments show that without good adhesion Al can flake away at the points of PP-film microhillocks that degrades selective properties of fabricated microstructures. In our case Ti-inclusive prototypes are devoid of such a drawback. However their manufacturing required to increase duration of a CPhLT's chemical etching stage results in slight augmentation of holes diameter *a*. The Table 1 resumes key information on four fabricated prototypes including measured values of actual hole diameter *a*. Figures 2(b)-(c) illustrate the microscopic structure of the fabricated samples by the example of the prototype #3. The images were obtained by optical microscopy in the "light reflection" regime with enhanced phase contrast. Light illumination and observer position correspond to the side of the PP-film (the Al-layer is located beneath the film). It is clearly seen the aforementioned residual granularity of low-cost commercial PP (Fig. 2(b)). The typical value of the microhillock height measured by refocusing from PP surface onto the microhillock's apex (Fig. 2(c)) appeared to be 8 μm. Presence of diffused background scattering in Fig. 2(c) points out at nonideal smoothness of the film.

#109149 - $15.00 USD Received 25 Mar 2009; revised 7 May 2009; accepted 3 Jun 2009; published 29 Jun 2009

3. Numerical and measurement results

We perform numerical simulations using the commercially available 3D electromagnetic solver CST Microwave Studio^{TM}, which is based upon Finite Integration Time Domain Method (FITD). We simulate a unit cell as shown in Fig. 2(a) with periodic boundary conditions in the directions perpendicular to the direction of propagation thus ensuring a correct periodic continuation of the structure. Along the propagation direction (z-axis), open boundary conditions are employed. A Drude model for metals is used: the plasma frequency for aluminium is $\omega_p = 2.243 \times 10^{16}$ rad/s and the collision frequency chosen is $\gamma = 3.4 \times 10^{14}$ Hz. The skin depth is $\delta_{sd} = (2/(\mu\omega\sigma))^{1/2}$ where μ is the magnetic permeability which is $4\pi \times 10^{-7}$ H/m in our case, and σ is the conductivity. Thus, for $\omega = 6.28 \times 10^{12}$ and 3.14×10^{13} rad/s (1 and 5 THz), the skin depth for Al is approximately 81.4 and 36.4 nm respectively. These values assure that the coupling between either face of EOT surface is through the subwavelength hole rather than evanescent waves through the metal within our frequency range. The dielectric constant of the PP was taken as $\varepsilon_r = 2.25$ with loss tangent $tg\delta = 0.001$, according to the experimental characterization of the previous section. Finally, a tetrahedral mesh was used and the desired linear equation system solver accuracy in terms of the relative residual normal was chosen as 10^{-9} and reached in all simulations.

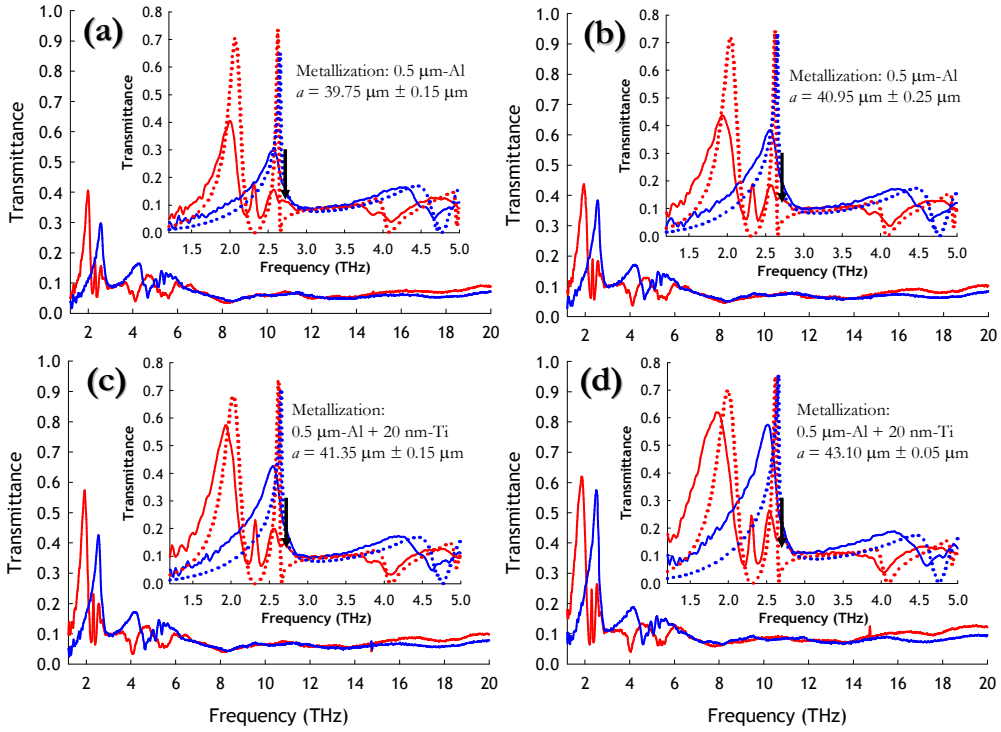

Fig. 3. Transmittance for p-polarzation (red curves) and s-polarization (blue curves) measurements. Dotted lines in the insets correspond to numerical results. Prototypes without Ti-layer: (a) hole diameter a = 39.75 μm, (b) a = 40.95 μm; Prototypes with Ti-layer: (c) a = 41.35 μm, (d) a = 43.10 μm. To guide the eye, black arrow indicate Wood's anomaly linked with the large periodicity in the interface air-metal.

Measurements were performed using the vacuum FT-spectrometer "Bruker IFS 66v/s". The frequency dependent THz intensity of the prototypes for both incident polarizations in the whole bandwidth is plotted in Fig. 3, whereas a zoom of the experimental Extraordinary Transmission peaks along with simulation results are displayed in corresponding insets of Fig. 3.

#109149 - $15.00 USD Received 25 Mar 2009; revised 7 May 2009; accepted 3 Jun 2009; published 29 Jun 2009

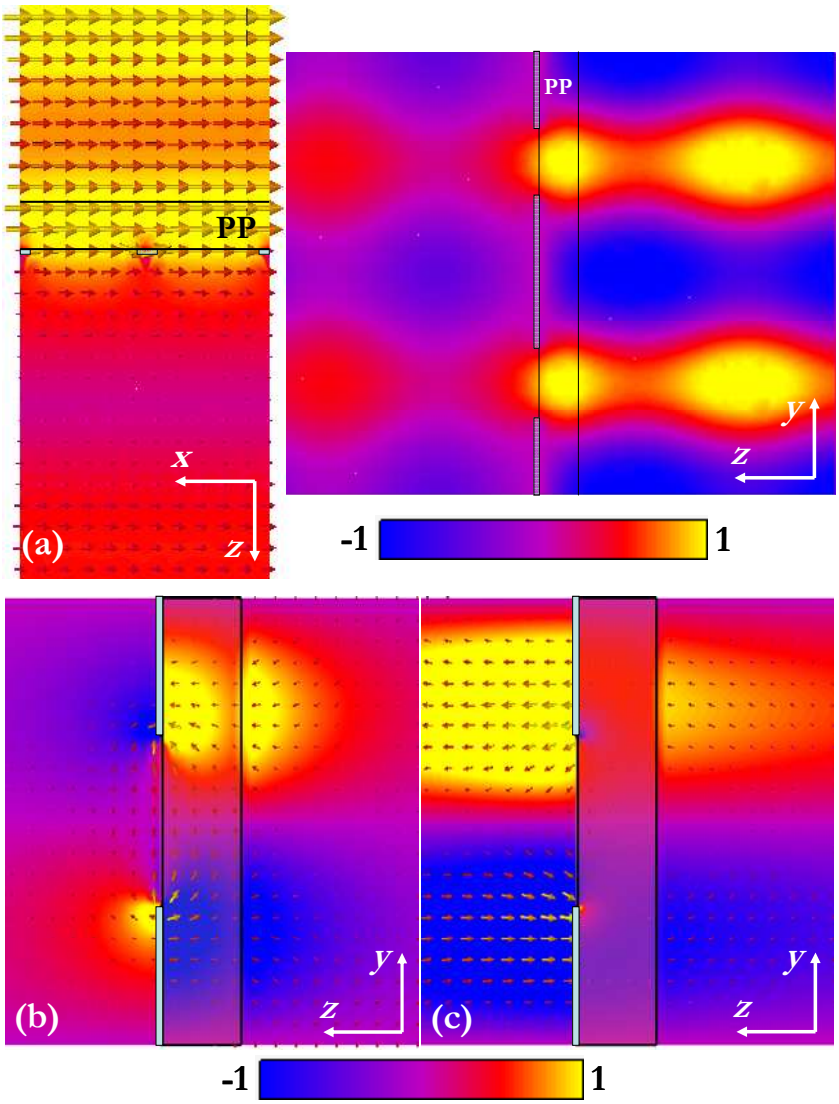

Fig. 4. (a) Cross-sectional views of the unit cell just in the middle of the hole of the electric field (arrows) – only in the left hand side panel - and x-component of the electric field E_x (color map), in the vicinity of the structure with geometrical parameters as prototype 1 under s-polarization. (b, c) Cross-sectional view of the electric field (arrows) and z-component of the electric field E_z (color map), in the vicinity of the structure under p-polarization: (b) lower frequency peak – antisymmetric coupling, (c) higher frequency peak – symmetric coupling.

For s-polarization (blue curves) EOT is not expected unless a thin dielectric slab on top of the metallic layer is placed [21] as in our prototypes. This anomalous maximum within the cutoff zone – the cutoff frequency of a single hole of radius 20.5 μm is f_{co} = 4.3 THz or 2.85 THz when is loaded with air or PP respectively – is around 2.55 THz in all prototypes with relatively high intensity values of 0.30, 0.38, 0.42, and 0.57 respectively and the Wood anomaly of the interface air-metal is around 6.3 THz for this case. The electric field distribution at the xz- and yz-planes corresponding to this anomalous peak is rendered in Fig. 4(a), where arrows point at the direction of the E-field, whereas color map illustrate the proportional magnitude of the x-component of it (y- and z-components are negligible. The z-component is only noticeable at the edge of the holes, see arrows). The incoming plane wave

#109149 - $15.00 USD Received 25 Mar 2009; revised 7 May 2009; accepted 3 Jun 2009; published 29 Jun 2009

seems to just accommodate to the holes so as to pass through them which are in accordance with Ref. 21 for subwavelength slit arrays.

In the case of p-polarization (incident electric field along the large periodicity of the hole array), E_y (red curves), the low frequency resonant response is originated from the antisymmetric combination of the two SPP-like modes associated with the two interfaces of the structure (so-called Short Range-SPP-like mode, SR-SPP-like mode), Fig. 4(b). This is straightforwardly derived from the opposite colours at each face of the metal layer in Fig. 4(b). Intensity of each prototypes is 0.41, 0.44, 0.57 and 0.62 corresponding to hole diameter a = 39.75, 40.95, 41.35 and 43.10 μm. Note that for both polarizations, the peak reaches similar amplitude values. The other resonance feature observed below Wood's anomalies within the cutoff region is caused by the corresponding symmetric combination (so-called Long Range-SPP-like mode, LR-SPP-like mode), Fig. 4(c). In this case, intensity values are 0.16, 0.18, 0.20 and 0.26 in that order. These measurements agree well with numerical results, where small discrepancies could be attributed to differences between the parameters used to model metals and PP-film and the real ones. Besides, in Figs. 4(b) and 4(c), where the field distribution at the *yz* incident plane is depicted (arrows point at the direction of the E-field, whereas color maps illustrate the proportional magnitude of the *z*-component of it), it is as well highlighted the higher confinement to the metal of the SR-SPP-like mode in opposition to LR-SPP-like mode, since the z-component of the electric field E_z associated with the surface wave prolongs significantly within the air region.

The experimental dependence on the size of the hole is plotted in Fig. 5 (dark blue dots for s-polarization, and black and red dots for usual EOT excitation), and is in accordance with similar studies, as well as numerical results (blue, and gray and pink dots for anomalous and common EOT respectively). As it was previously reported for subwavelength hole arrays in the visible [25], the increase of the size of the holes shifts the resonance frequencies related to SR- and LR-SPP-like modes toward lower frequencies, although this is more pronounced for the SR-like mode case. An intuitive idea is based on the fact that the bigger the hole, the lower the frequency cutoff. Therefore, the spectrum governed by the subwavelength holes, that is, the EOT, may shift to allow transmission, but Wood's anomalies must remain in the same frequency since it depends on the lattice constant. As a result of the last fact, and recalling that the LR-like mode emerge close to air-metal Wood's anomaly minimum, this explain the less pronounced shift undergone by the LR-like mode. With regards to the anomalous EOT peak, its behaviour seems to follow LR-like mode because of its emergence near the air-metal Wood's anomaly as Ref. 21 suggests.

5. Conclusion

Anomalous Extraordinary Optical Transmission in subwavelength hole arrays deposited over a PP-substrate is experimentally demonstrated at the so-called THz-gap. Contrary to standard EOT which is explained by the so-called spoof plasmons substantiated both in free-standing and dielectric embedded structures, this EOT for s-polarization arises from surface waves supported by the thin PP layer (that is, in dielectric embedded structures). As a point of interest, we have experimentally found that the amplitude the anomalous peak is similar to the amplitude of the standard EOT SR-SPP-like mode. This result is based on the design and manufacture by contact photolithography of a low-cost but accurate Extraordinary Transmission doubly periodic subwavelength hole array within the so-called THz-gap. Moreover, particular attention is paid to wideband characterization of the PP-substrate used. Both symmetric and antisymmetric modes of the usual EOT are reported and experimental results agree well with numerical analysis and with literature devoted to EOT in other frequencies ranges. These results could find application in the design of novel THz and optical devices like filters and polarisers.

#109149 - $15.00 USD Received 25 Mar 2009; revised 7 May 2009; accepted 3 Jun 2009; published 29 Jun 2009

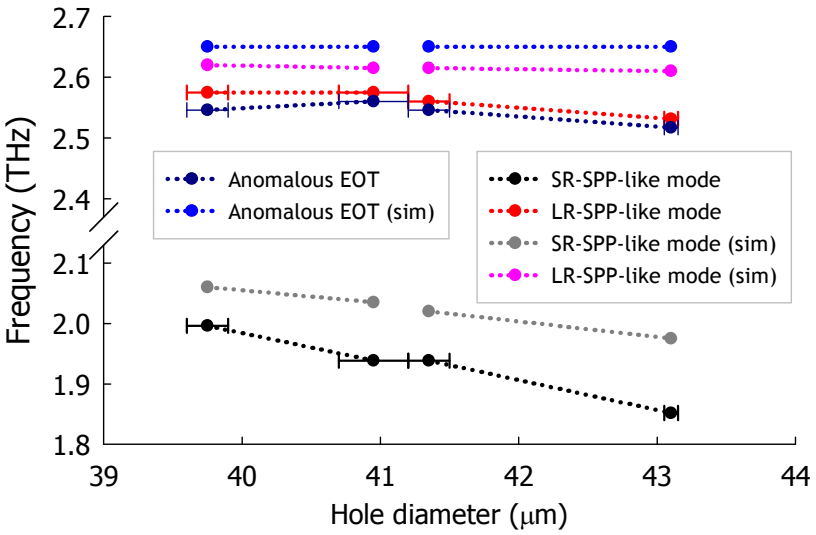

Fig. 5. Peak frequency as a function of the hole diameter; (black) lower frequency resonance, (red) higher frequency resonance, (gray) and (pink) for numerical results in that order. The dotted lines are guides to the eyes.

Acknowledgements

This work was supported by Spanish Government and E.U. Feder under contracts Consolider "Engineering Metamaterials" CSD2008-00066 and TEC2008-06871-C02-01.

#109149 - $15.00 USD Received 25 Mar 2009; revised 7 May 2009; accepted 3 Jun 2009; published 29 Jun 2009